Worldwide site comparison for submillimetre astronomy

Pascal Tremblin, N. Schneider, V. Minier, G. Al. Durand, Jakub Urban

▶ **To cite this version:**

Pascal Tremblin, N. Schneider, V. Minier, G. Al. Durand, Jakub Urban. Worldwide site comparison for submillimetre astronomy. Astronomy and Astrophysics - A&A, 2012, 548, pp.id.A65. 10.1051/0004-6361/201220420 . hal-00839145

HAL Id: hal-00839145
https://hal.science/hal-00839145

Submitted on 7 Jan 2023

HAL is a multi-disciplinary open access archive for the deposit and dissemination of scientific research documents, whether they are published or not. The documents may come from teaching and research institutions in France or abroad, or from public or private research centers.

L'archive ouverte pluridisciplinaire **HAL**, est destinée au dépôt et à la diffusion de documents scientifiques de niveau recherche, publiés ou non, émanant des établissements d'enseignement et de recherche français ou étrangers, des laboratoires publics ou privés.

A&A 548, A65 (2012)
DOI: 10.1051/0004-6361/201220420
© ESO 2012

Astronomy & Astrophysics

Worldwide site comparison for submillimetre astronomy

P. Tremblin[1], N. Schneider[1,2], V. Minier[1], G. Al. Durand[1], and J. Urban[3]

[1] Laboratoire AIM Paris-Saclay, CEA/Irfu – Univ. Paris Diderot – CNRS/INSU, Centre d'études de Saclay, 91191 Gif-Sur-Yvette, France
e-mail: pascal.tremblin@cea.fr
[2] Université de Bordeaux1, LAB, UMR 5804, CNRS, 33270 Floirac, France
[3] Chalmers University of Technology, Department of Earth and Space Sciences, 41296 Göteborg, Sweden

Received 20 September 2012 / Accepted 16 October 2012

ABSTRACT

Aims. The most important limitation for ground-based submillimetre (submm) astronomy is the broad-band absorption of the total water vapour in the atmosphere above an observation site, often expressed as the precipitable water vapour (PWV). A long-term statistic on the PWV is thus mandatory to characterize the quality of an existing or potential site for observational submm-astronomy. In this study we present a three-year statistic (2008–2010) of the PWV for ground-based telescope sites all around the world and for stratospheric altitudes relevant for SOFIA (Stratospheric Observatory for Far-Infrared Astronomy). The submm-transmission is calculated for typical PWVs using an atmospheric model.

Methods. We used data from IASI (Infrared Atmospheric Sounding Interferometer) on the Metop-A satellite to retrieve water vapour profiles for each site (11 in total, comprising Antarctica, Chile, Mauna Kea, Greenland, Tibet). The use of a single instrument to make the comparison provides unbiased data with a common calibration method. The profiles are integrated above the mountain/stratospheric altitude to get an estimation of the PWV. We then applied the atmospheric model MOLIERE (Microwave Observation and LIne Estimation and REtrieval) to compute the corresponding atmospheric absorption for wavelengths between 150 μm and 3 mm.

Results. We present the absolute PWV values for each site sorted by year and time percentage. The PWV corresponding to the first decile (10%) and the quartiles (25%, 50%, 75%) are calculated and transmission curves between 150 μm and 3 mm for these values are shown. The Antarctic and South-American sites present very good conditions for submillimetre astronomy. The 350 μm and 450 μm atmospheric windows are open all year long, whereas the 200 μm atmospheric window opens reasonably for 25% of the time in Antarctica and the extremely high-altitude sites in Chile. Potential interesting new facilities are Macon in Argentina and Summit in Greenland, which show similar conditions to for example, Mauna Kea (Hawaii). For SOFIA, we present transmission curves for different altitudes (11 to 14 km), PWV values, and higher frequencies (up to 5 THz) in more detail. Though the atmosphere at these altitude is generally very transparent, the absorption at very high frequencies becomes more important, partly caused by minor species. The method presented in this paper could identify sites on Earth, with great potential for submillimetre astronomy, and guide future site testing campaigns in situ.

Key words. site testing – submillimeter: general

1. Introduction

Despite its strong interest for astronomy, the submillimetre (submm) to far-infrared (FIR) wavelength range is mostly limited by the pressure-broadened absorption of tropospheric water vapour present in the Earth's atmosphere (see, e.g., Minier et al. 2010, for a summary of astronomy projects). The water vapour profile, and thus also the integrated column of water expressed in precipitable water vapour (PWV), depends on the geographical location. The PWV generally decreases with altitude, so that high-lying sites are best suited to submm-astronomy. Airborne astronomy, now possible on a regular base using SOFIA, is much less limited by water vapour, and thanks to the lower atmospheric pressure, spectral broadening is less important. However, there is still absorption close to major and minor species (e.g., O_3, N_2O, CO), as well as collision-induced non-resonant continuum absorption. SOFIA can now access the very high-frequency range (>2 THz), definitely closed for ground-based sites, but the line intensities and abundances of the major and minor species need to be known precisely. First spectroscopic observations performed with SOFIA (see A&A special issue, 2012, vol. 542) show that small-scale atmospheric variations in the troposphere/stratosphere layer are very difficult to assess (Guan et al. 2012).

For ground-based sites, previous studies (e.g. Schneider et al. 2009; Tremblin et al. 2011; Matsushita et al. 1999; Peterson et al. 2003) have already shown that a few sites are well-suited to submm/mid-IR, and FIR-astronomy and their transmission properties are rather well determined (for example by Fourier transform spectrometer obervations in the 0.5–1.6 THz range at Mauna Kea/Hawaii; Pardo et al. 2001). The high-altitude (>5000 m) Chilean sites are known for dry conditions (see Matsushita et al. 1999; Peterson et al. 2003), and site testing is now being carried out at the driest place on Earth, Antarctica (see Chamberlin et al. 1997; Yang et al. 2010; Tremblin et al. 2011). Comparisons between Antarctic and Chilean sites are difficult and uncertain since they rely on ground-based instruments that use different methods and calibration techniques (see Peterson et al. 2003, for example). The working conditions are also an important concern, since a single instrument moved from Chile to Antarctica will behave differently in the harsh polar environment (–70 °C in winter at Dome C). A meaningful comparison is possible if several independent instruments are used at each place. An example of such a study is the one of Tremblin et al. (2011)

that obtained transmission data at Dome C thanks to radio soundings and the radiometers HAMSTRAD (Ricaud et al. 2010) and SUMMIT08. However, it is rare to have many instruments at one site. The best solution is to use satellite data, which also enables any location on Earth to be investigated. Thanks to the IASI (Infrared Atmospheric Sounding Interferometer) on the Metop-A satellite, it is now possible to conduct such a comparison over several years with no instrument bias and with the same working conditions for the detectors. We present here a three-year study of the PWV of a selection of existing and upcoming submm-sites in Antarctica, Chile, Tibet, and Argentina, as well as for two SOFIA stations, Palmdale/California and Christchurch/New Zealand. The individual and cumulated quartiles of PWV for each site allow a direct comparison. The transmission corresponding to these PWV values of the quartiles is then calculated using the atmospheric model MOLIERE-5 (Microwave Observation and LIne Estimation and REtrieval, Urban et al. 2004).

The paper is organized as follows. After introducing all the sites that are considered in the present study (Sect. 2), we first show the PWV extraction from the satellite data and the comparison of the PWV statistics between all the sites (Sect. 3). Then we present the method extracting transmission curves with the MOLIERE atmospheric model and perform a site comparison for the 250 μm and 350 μm transmission (Sect. 4). The ratio of the monthly-averaged transmission to its fluctuations is then used to compare the stability of the transmission at 200 μm between all the sites at the end of Sect. 4. Section 5 deals with the results for SOFIA, and Sect. 6 discusses and summarizes the results.

2. Sites of interest

We selected eleven representative sites around the world that can be grouped as follows:

- *Antarctic sites.*
  Dome C: Concordia station with several telescopes, e.g. IRAIT (International Robotic Antarctic Infrared Telescope), http://arena.oca.eu;
  Dome A: new site in exploration, http://www.chinare.gov.cn;
  South Pole: SPT (South Pole Telescope), http://astro.uchicago.edu/research/south-pole-telescope.
- *South-American sites.*
  Chajnantor Plateau in Chile: ALMA (Atacama Large Millimetre Array) site, http://www.almaobservatory.org;
  Cerro Chajnantor in Chile: CCAT (Cornell Caltech Atacama Telescope), http://www.ccatobservatory.org;
  Cerro Macon in Argentinia.
- *Northern-hemisphere sites.*
  Mauna Kea in Hawaii: JCMT (James Clerk Maxwell Telescope), http://www.jach.hawaii.edu;
  Summit in Greenland: http://www.geosummit.org;
  Yangbajing in Tibet: KOSMA (Cologne Observatory for submm-astronomy), http://www.astro.uni-koeln.de/kosma.
- *"Stratospheric" sites.*
  SOFIA over Palmdale (USA) and Christchurch (New Zealand), http://www.sofia.usra.edu.

The location of the different sites are summarized in Fig. 1. Our selection inclues known sites in Antarctica and North/South America plus northern hemispheric sites that could be of interest (Summit in Greenland, Yangbajing in Tibet) for complete sky coverage. The geographical location, altitude, and related existing/planned telescopes are listed in Table 1.

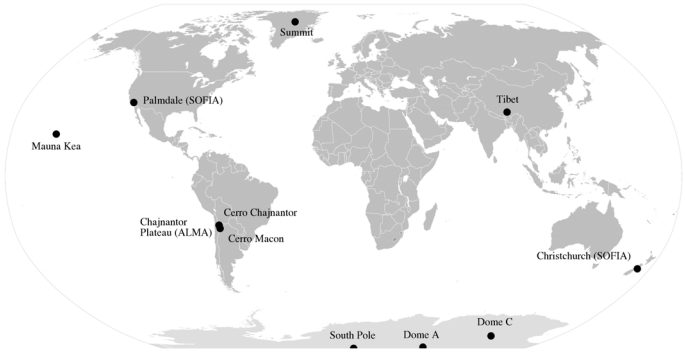

Fig. 1. Location of the different sites of interest.

Table 1. Location, altitude, and telescopes for the different sites with future telescopes indicated in parenthesis.

Site	Latitude	Longitude	Alt. [m]	Tel.
Dome C	75°06′s	123°23′e	3233	IRAIT
Dome A	80°22′s	77°21′e	4083	
South Pole	90°s	0°e	2800	SPT
Cerro Chajnantor	22°59′s	67°45′w	5612	(CCAT)
Cerro Macon	24°31′s	67°21′w	5032	
Chaj. Plateau	23°00′s	67°45′w	5100	ALMA
Mauna Kea	19°45′n	155°27′w	4207	JCMT
Summit, Greenland	72°35′n	38°25′w	3210	
Yangbajing, Tibet	30°05′n	90°33′e	4300	KOSMA
Palmdale	34°37′n	118°05′w	12 000	SOFIA
Christchurch	43°31′s	172°38′e	12 000	SOFIA

3. PWV extraction from satellite data

3.1. Method and results

IASI (Infrared Atmospheric Sounding Interferometer) is an atmospheric interferometer working in the infrared, launched in 2006 on the METOP-A satellite (Phulpin et al. 2007; Pougatchev et al. 2008; Herbin et al. 2009; Clerbaux et al. 2009). The data are available at the website of the Centre for Atmospheric Chemistry Products and Services[1]. IASI was developed by the French Space Agency CNES[2] in collaboration with EUMETSAT[3]. The satellite is on a polar orbit so that each point on Earth is seen at least once per day by the detectors. IASI is a Fourier transform spectrometer (FTS) working between 3.7 and 15.5 μm. It is associated with an infrared imager, operating between 10.3 and 12.5 μm. Each pixel of the instrument corresponds to a spatial extent of 12 km at nadir, and vertical profiles of tropospheric humidity at ninety pressure levels are retrieved typically with 10% accuracy (Pougatchev et al. 2008). The amount of precipitable water vapour is given by the integral of these vertical profiles. We averaged, on a daily basis all measurements whose central position falls in a zone of 110 km^2 around each site to derive PWV statistics between 2008 and 2010. This method was

[1] http://ether.ipsl.jussieu.fr
[2] Centre National d'Études Spatiales.
[3] European organization for meteorological satellites http://www.eumetsat.int

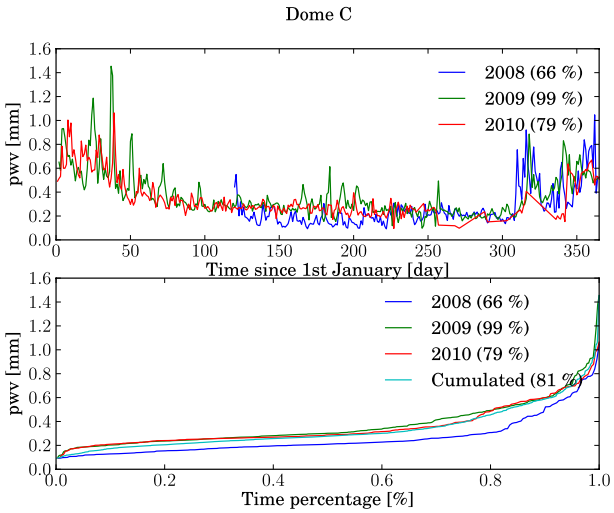

Fig. 2. *Top*: PWV content measured at Dome C, Antarctica over the French-Italian base Concordia between 2008 and 2010. The percentage indicates the fraction of days in the year when we were able to extract the data from the satellite measurements. *Bottom*: distribution function of the PWV for each year and for the whole period.

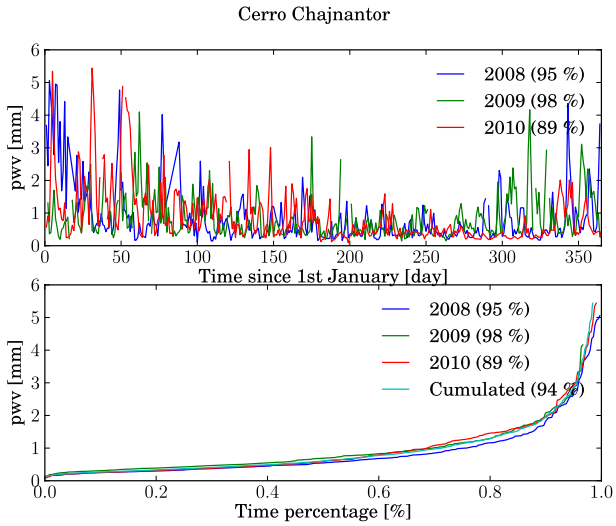

Fig. 3. Same as Fig. 2 for Cerro Chajnantor in Chile. The satellite profiles were truncated at the altitude of the mountain summit. Note the different scale range of PWV compared to Fig. 2.

validated in Tremblin et al. (2011) where we compared IASI satellite data with ground-based instruments (HAMSTRAD and SUMIT08) and radio-sounding data over the French-Italian base Concordia at Dome C in Antarctica. All instruments have a good correlation at low PWV, which is precisely the range we are interested in for submillimetre astronomy.

The use of vertical satellite profiles is slightly trickier for a mountain site. Since we take all measurements in a zone of 110 km^2, we sometimes get profiles that do not contain mountain altitude but include lower ones. This would bias the retrieved PWV to high values. To overcome this difficulty, we generally truncated the profiles at the pressure level of the site of interest. This method has already been used by Ricaud et al. (2010) to compare IASI measurements with the HAMSTRAD radiometer, over the Pyrenees mountains. They showed a very good correlation for the integrated PWV. We also determined the PWV content in this way at high altitudes (>11 km) over Palmdale, USA, and Christchurch, New Zealand, for the on-going and future flights of SOFIA. During a typical flight, SOFIA will range hundreds of kilometres from its base and the water vapour depends on local weather conditions at the position of the plane. Since the profiles are averaged on a 110-km^2 area and the time statistics are done for three years, the results given here are the representative conditions under which SOFIA is operating. Precise in-situ measurements of the PWV usable for calibration are much more difficult to obtain (see Guan et al. 2012).

The water vapour profiles are measured as a function of pressure by IASI, therefore it is important to get the correct pressure level at the altitude of the sites. In-situ measurements were available for most of the sites to get the local averaged pressure level. Only for Yangbajing, Cerro Macon, and SOFIA was it necessary to use the pressure level of the standard US atmosphere (1976), computed at the altitude of the site. However, this method does not provide a precise pressure level, just a measured one, so that the retrieved PWVs are less reliable. By comparing both methods for sites where measurements were available, we estimate an error of around 25 % using the standard atmosphere.

Figure 2 presents the PWV measurements for the Antarctic site of Dome C and Fig. 3 the measurements for the Chilean site of Cerro Chajnantor. The corresponding figures for all other sites are found in the Appendix and on a dedicated website[4]. Since on Antarctic domes (expression for the mountains in Antarctica), the difference in height is small (over 100 km), we do not need to truncate the profiles, whereas it has to be done for a mountain site like Cerro Chajnantor.

Some ground measurements are available for different sites and can be compared to our results. Cerro Chajnantor and Chajnantor Plateau were extensively studied (see Giovanelli et al. 2001) and the PWV quartiles between 2006 and 2010 can be found in Radford (2011). The values deduced from opacity measurements at 225 GHz are 0.61 mm (25%), 1.08 mm (50%), and 2.01 mm (75%) for the plateau; and 0.33 mm (25%), 0.61 mm (50%), and 1.36 mm (75%) for Cerro Chajnantor. The quartiles for Cerro Chajnantor are in a good agreement with our satellite measurements (between 10 and 20% difference). The studied periods are not the same and can explain partly the difference. Furthermore, a scale height of the water vapour profiles on the Chajnantor area can be deduced from the quartiles of the plateau and the "Cerro". With the satellite measurements, we computed a 1/e scale height h_e of the order of 1.1 km that is in a good agreement with measurements from Giovanelli et al. (2001). The PWV quartiles at the South Pole were computed at saturation from radio-sounding balloons over a period of 40 years (see Chamberlin 2002). These authors estimate that the PWV should be 90% saturated, thus the saturation level can be used as a proxy for the real PWV. They find averaged quartiles of 0.25 mm (25%), 0.33 mm (50%), and 0.44 mm (75%); the difference with our satellite measurements is around 10%. A radiometer at 225 GHz is operating at the CSO[5] on Mauna Kea. PWV quartiles between 1997 and 2001 can be found in Otárola et al. (2010) and Radford (2011), 1.08 mm (25%), 1.82 mm (50%), and 3.32 mm (75%). The difference with the satellite measurements is around 15–20% and can again be caused by variations between the periods 1997–2001 and 2008–2010.

The effect of seasons are clearly visible in Figs. 2 and 3. Obviously, the PWV during winter is lower than in summer, i.e., below 0.3 mm at Dome C and below 0.6 mm at Cerro Chajnantor. The Chilean site presents a strong day-to-day

[4] http://submm.eu
[5] Caltech Submillimeter Observatory.

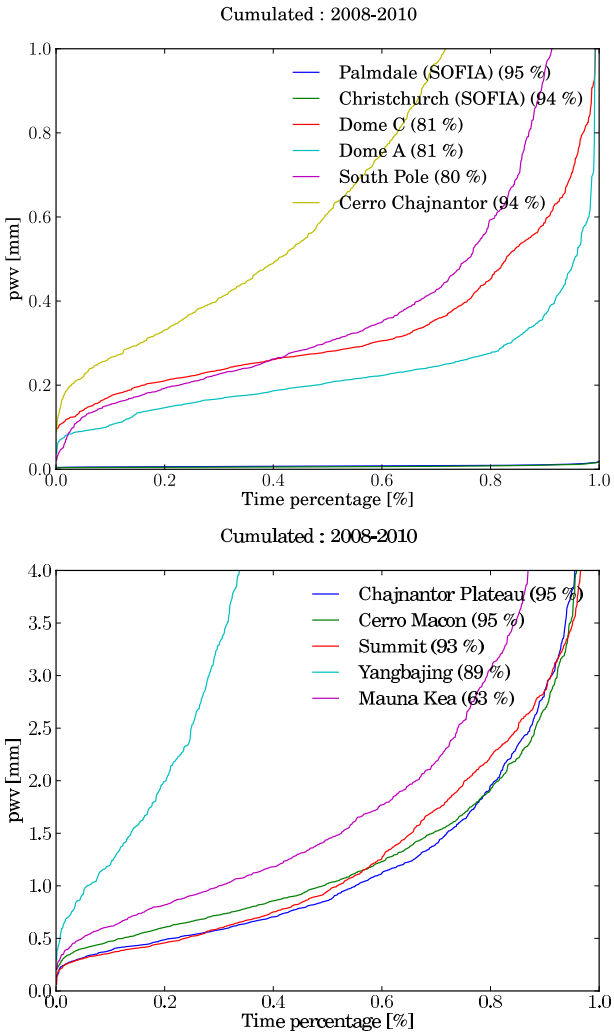

Fig. 4. Comparison of the distribution functions of the PWV for all sites between 2008 and 2010. The percentage of days over this period on which we achieved the data extraction is indicated in parenthesis. The time percentage (x-axis) is taken over the total number of days on which we achieved the data extraction. In the *upper panel*, the curves for Palmdale (dark blue) and Christchurch (green) are blended and very close to the 0.0 mm level.

variation compared to the Antarctic site. This is caused by the daily variation in the PWV that is not present in Antarctica with the long polar night/winter. This may cause a slight bias in the non-polar site data because only one or two measurements are available per day, thus we do not sample these day-night variations very well. Nevertheless, we expect these statistics to represent the trends over years. The distribution functions in Fig. 3 are very similar from 2008 and 2010, therefore the year-to-year statistics are not too affected by the lack of the day-night variation sampling. In 2008 the PWV was slightly lower than in 2009–2010. This effect was also seen in Antarctica (see Fig. 2) with the in-situ measurements (radio-soundings, HAMSTRAD, SUMMIT08). Possible explanations were discussed in Tremblin et al. (2011) and should not be interpreted as a possible effect of the day-night variations.

3.2. Site comparison

Figure 4 shows the comparison between all sites as a distribution function of the PWV over the period 2008–2010. Obviously, the air-borne SOFIA stratospheric instrument encounters the lowest PWV, lower than 0.01 mm most of the time and much lower than any ground-based sites. The Antarctic sites follow then as the driest places on Earth, with Dome A, and then Dome C and the South Pole. These sites have PWVs that are lower than 0.5 mm most of the time (75% of the time between 2008 and 2010). Chilean and Argentinian sites are next with a PWV lower than 1.5 mm most of the time, followed by Hawaii and Summit in Greenland with a PWV lower than 2 mm, and finally Yangbajing in Tibet, which presents a high level of water vapour. The satellite measurements saturate over the Tibet site with high values of the PWV (around 10 mm), which is clearly visible in the figure in the appendix.

These results are presented quantitatively in Table 2 with the first decile and the quartiles for each site. The difference caused by the truncation for mountain sites can be seen by comparing Cerro Chajnantor to Chajnantor Plateau. The mountain (Cerro) is close to the ALMA site, therefore the profiles that are extracted from the satellite are the same. The difference in the PWV retrieved is mostly caused by the altitude truncation of the profiles. The first decile and the quartiles again clearly show that Antarctic sites are the driest sites followed by South American sites and then northern hemisphere sites. It is remarkable that our long-term satellite statistics of PWV show that the site of Summit in Greenland offers comparable observing conditions (PWV and altitude) like the ones on Mauna Kea, which opens a new perspective for submm astronomy in the northern hemisphere.

4. Atmospheric transmission from PWV and MOLIERE

4.1. Method

For determining of the tropospheric transmission corresponding to the PWVs of the various deciles and quartiles for each site, we use *MOLIERE-5.7*, a forward and inversion atmospheric model (Urban et al. 2004), developed for atmospheric science applications. It has previously been used to calculate the atmospheric transmission up to 2000 GHz (~150 μm) for a large number of astronomical sites. The results are published in Schneider et al. (2009) and on a website[6].

The code calculates the absorption of radiation in the mm- to far-IR wavelength range (equivalent from 0 to 10 THz in frequency) considering the wet- and dry-air components of atmospheric absorption. Spectroscopic lines, such as those of atmospheric water (H_2O), oxygen (O_2), and ozone (O_3), absorb strongly at short wavelengths, while collisions of H_2O with O_2 and nitrogen (N_2) result in continuous absorption across all wavelengths. For the line absorption, a radiative transfer model including refraction and absorption by major and minor atmospheric species is included (H_2O, O_2, O_3, NO_2, HNO_3, CO and other lines up to 10 THz). Spectroscopic parameters are taken from HITRAN[7] and the JPL[8] database. The wet and dry air continuum absorption is calculated as described in Schneider et al. (2009). Temperature and pressure profiles of the sites were determined using the compilation described in Schneider et al. (2009) and given on the website. The colder Antarctic atmosphere tends to populate the low-lying energy state of water, leading to a greater absorption for a given PWV than that of a non-polar site. This effect is included in the model.

[6] http://submm.eu
[7] High Resolution Transmission molecular absorption database.
[8] Jet Propulsion Laboratory.

Table 2. First decile and quartiles of the PWV for all the studied sites.

Time fraction 2008–2010	SOFIA (Palm./Christ.)	Dome A	Dome C	South Pole	Cerro Chajnantor
0.10	0.006/0.004	0.11	0.17	0.15	0.27
0.25	0.006/0.005	0.16	0.22	0.21	0.37
0.50	0.007/0.006	0.21	0.28	0.30	0.61
0.75	0.009/0.007	0.26	0.39	0.49	1.11
Time fraction 2008–2010	Chajnantor Plateau	Summit	Cerro Macon	Mauna Kea	Yangbajing
0.10	0.39	0.36	0.47	0.62	1.21
0.25	0.53	0.51	0.66	0.91	2.47
0.50	0.86	0.94	1.02	1.44	inf
0.75	1.63	1.96	1.66	2.57	inf

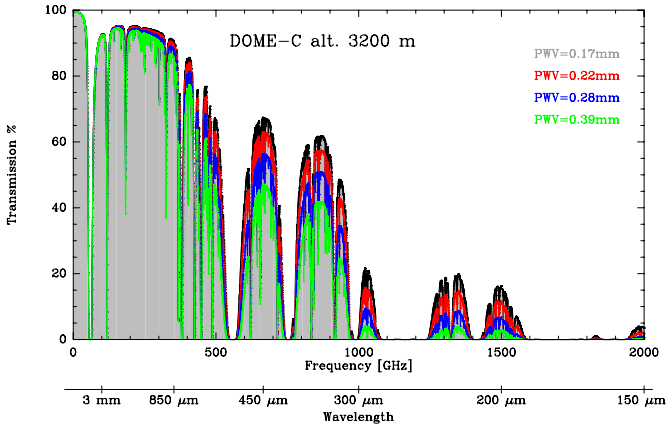

Fig. 5. Transmission curves between 150 μm and 3 mm corresponding to the first decile (grey) and the quartiles (red: 25%, blue: 50%, green: 75%) of PWV between 2008 and 2010 at Dome C.

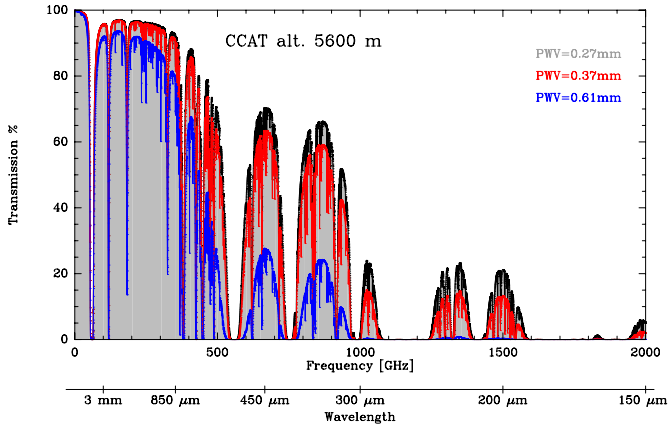

Fig. 6. Transmission curves between 150 μm and 3 mm corresponding to the first decile (grey) and the quartiles (red: 25%, blue: 50%) of PWV between 2008 and 2010 at Cerro Chajnantor.

We present here the transmission curves corresponding to the first decile and the quartiles of PWV for two sites of currently strong interest, Dome C (Fig. 5) and Cerro Chajnantor (Fig. 6), while transmission curves for the other sites are found in the appendix. From Table 2 we find that Dome C shows generally lower PWV values than Cerro Chajnator for longer time periods. Comparing the transmission curves at the same PWV (for example, 0.28/0.27 mm, which corresponds to 50% of the time at Dome C – blue curve – and 10% of the time at Cerro Chajnator – grey line) indicates, however, that the transmission is slightly higher at Cerro Chajnator. It corresponds to 20 (65)% at 200 μm (350 μm) for Cerro Chajnator with regard to ∼10 (60)% at 200 μm (350 μm) for Dome C. The difference becomes more important for high frequencies (shorter wavelengths) because the absorption by water vapour and the dry-air component are both a function of the altitude. See Schneider et al. (2009) for more details on the different absorption characteristics that depend on altitude and wavelength. In any case, observations at 350 and 450 μm are possible all year long for both observatories.

4.2. Site comparison

Based upon the method described in Tremblin et al. (2011), we use MOLIERE to calculate the transmissions at 200 μm and 350 μm. We do not compute the transmissions for SOFIA here because it is by far superior to all ground-based sites. Its transmission curves are discussed in a dedicated section (Sect. 5).

Figure 7 shows the distribution functions of the 350- and 200-μm transmissions for all the other sites. In Table 3, we give the first decile and the quartiles of 200- and 350-μm transmissions. 25% of the time, a transmission better than 55–65% (10–20%) at 350 μm (200 μm) can be found in Antarctica. For the first quartile, Cerro Chajnantor catches up the Antarctic sites thanks to its high altitude; however for the second and third quartile Antarctic sites have better transmissions based on the long-term statistics, especially at 350 μm. For the three sites, Chajnantor Plateau, Cerro Macon, and Mauna Kea, the transmission window at 350 μm opens significantly, while it is only rarely possible to observe at 200 μm.

The extreme stability of the Antarctic sites is clearly visible in Fig. 7. There is a stable plateau for the transmission between the first and third quartiles that allows long time series and surveys to be conducted on these sites. This is the direct consequence of the stability of the PWV that was previously identified at Dome C in Fig. 2. With its higher altitude, Dome A presents the best conditions on Earth for submillimetre astronomy in terms of transmission and day-to-day stability.

4.3. Transmission stability at 200 μm

The stability of the transmission is an important parameter for large surveys and time-series studies. The PWV of Chilean sites is highly variable from one day to the next, whereas Antarctic sites are much more stable (see Figs. 2 and 3). The stability of the transmission leads to a high transmission even at long time fraction in the distribution functions of Fig. 7. To quantify and compare the stability, we used the indicator introduced by De Gregori et al. (2012), the site photometric quality ratio (SPQR). It consists in the ratio of the monthly averaged

Table 3. First decile and quartiles of the 350-μm (*top*) and 200-μm (*bottom*) transmissions for all the studied sites.

Time fraction 2008–2010	Dome C	Dome A	South Pole	Cerro Chaj.	Chaj. Plat.	Cerro Macon	Mauna Kea	Summit	Yangbajing
0.10	0.62	0.72	0.61	0.65	0.56	0.49	0.40	0.42	0.19
0.25	0.57	0.67	0.56	0.58	0.46	0.41	0.27	0.31	0.02
0.50	0.51	0.62	0.47	0.44	0.31	0.29	0.14	0.15	0.00
0.75	0.41	0.57	0.34	0.24	0.12	0.15	0.03	0.02	0.00
Time fraction 2008–2010	Dome C	Dome A	South Pole	Cerro Chaj.	Chaj. Plat.	Cerro Macon	Mauna Kea	Summit	Yangbajing
0.10	0.17	0.32	0.16	0.20	0.09	0.05	0.03	0.03	0.00
0.25	0.11	0.22	0.11	0.12	0.04	0.02	0.01	0.01	0.00
0.50	0.07	0.16	0.05	0.04	0.01	0.00	0.00	0.00	0.00
0.75	0.03	0.11	0.01	0.00	0.00	0.00	0.00	0.00	0.00

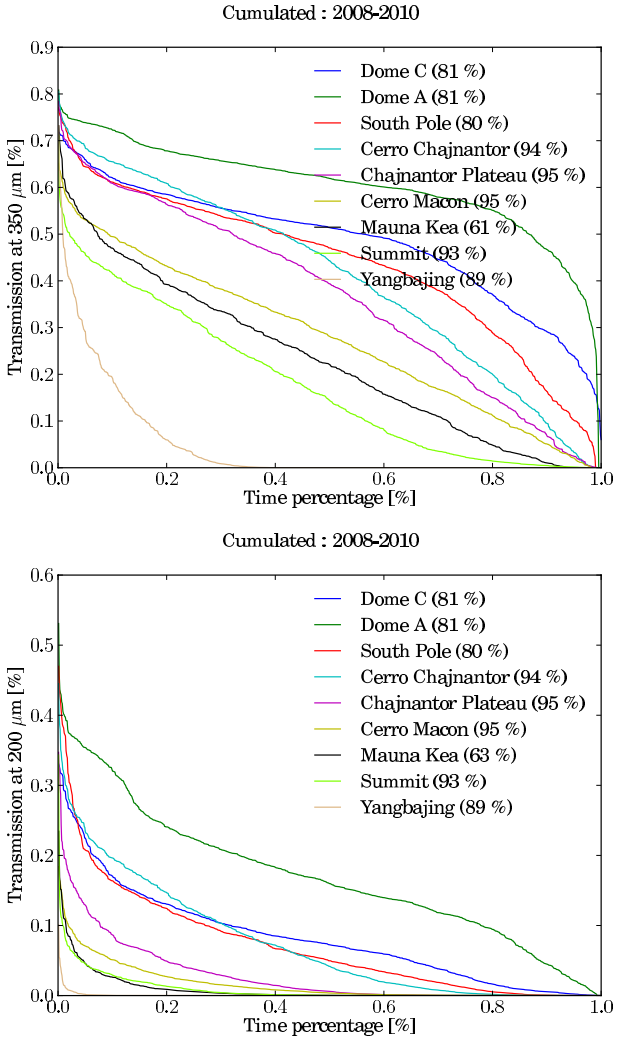

Fig. 7. Comparison of the distribution functions of the 350-μm (*top*) and 200-μm (*bottom*) transmissions for all the sites between 2008 and 2010. The x-axis time percentage is done over the period during which the data extraction for the sites was possible, the actual percentage of data we got is indicated for each site in parenthesis.

transmission to its monthly standard deviation, on a daily time scale

$$\mathrm{SPQR} = \langle T \rangle / \sigma_T. \quad (1)$$

The variations in this ratio for the transmission at 200 μm between 2008 and 2010 are plotted in Fig. 8, and they indicate

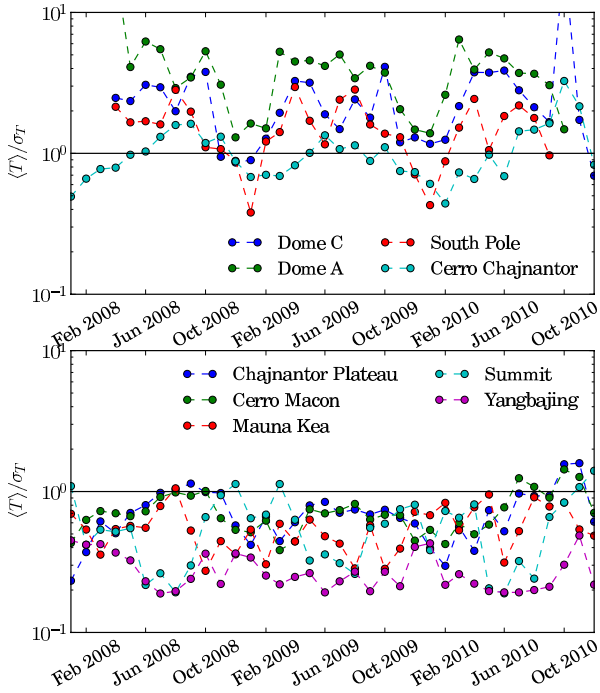

Fig. 8. SPQR ratio for the 200-μm transmission for all the sites between 2008 and 2010. The mean values between 2008 and 2010 are Dome A 3.6, Dome C 2.7, South Pole 1.3, Cerro Chajnantor 1.1, Chajnantor Plateau 0.7, Cerro Macon 0.7, Mauna Kea 0.6, Summit (Greenland) 0.6, and Yangbajing (Tibet) 0.3.

that all temperate sites have an SPQR ratio lower than 1, while Antarctic sites have a ratio greater than 1. Therefore, the fluctuations of the transmission are greater than the averaged transmission, on temperate sites. This quantifies the high variability of the transmission at these sites. The Arctic site on the Summit mountain is also highly variable, so that Antarctica is really unique even among polar environments. On the Antarctic plateau, Dome A has the best SPQR ratio with a monthly averaged transmission that is typically three to four times higher than the fluctuations. Dome C also achieves very good conditions with a ratio of 2–3, while the South Pole has a monthly-averaged transmission of the same order as the fluctuations, so comparable to the conditions reached at Cerro Chajnantor.

5. Atmospheric transmission for SOFIA

The first successful science flights with SOFIA were carried out in 2011 and are summarized in special issues of A&A (2012,

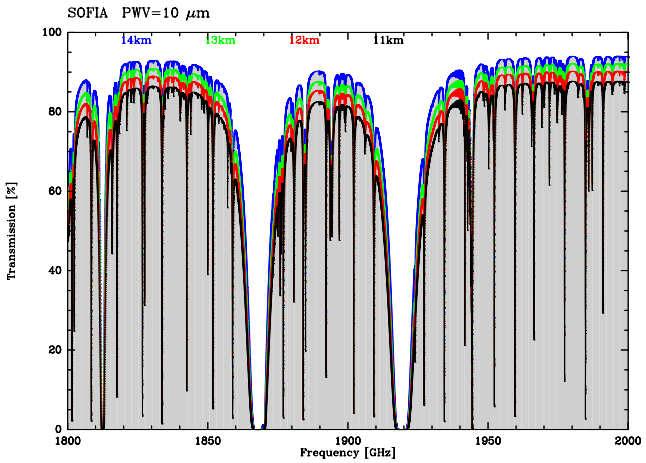

Fig. 9. Atmospheric transmission curve for 4 flight altitudes of SOFIA calculated with MOLIERE at a PWV of 10 μm.

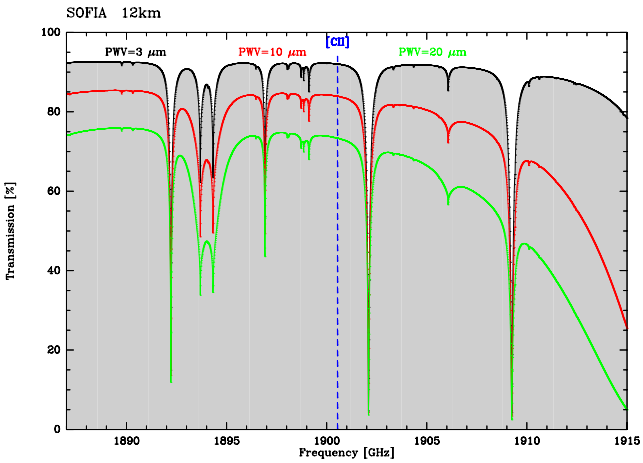

Fig. 10. Zoom into the transmission curve for the frequency range containing the [CII] 1.9 THz for 3 different PWV at an altitude of 12 km calculated with MOLIERE. The [CII] line is indicated by a dashed blue line.

Vol. 542, spectroscopic observations with GREAT) and ApJ (2012, Vol. 749, continuum imaging). In particular, the spectroscopic observations at high frequencies (e.g. the [CII] line at 1.9 THz) showed that, although the transmission is very high at these frequencies (typical PWVs are in the range of a few μm up to 50 μm for altitudes between 11 and 14 km), the calibration of the data using atmospheric models is not straightforward and requires a more detailed understanding of the atmospheric processes at the troposphere/stratosphere border. As pointed out in Guan et al. (2012), atmospheric models are particularly important because atmospheric absorption lines are narrower at these altitudes, and their small-scale variation is very difficult to measure. In Guan et al. (2012), three atmospheric models are compared: AM (Paine 2011), ATRAN (Lord 1992, priv. comm.), and MOLIERE (Urban et al. 2004). Special emphasis is given separately to the wet and dry components. While all models agree well for the wet component, ATRAN does not include the collision-induced absorption by N_2 and O_2, and AM calculates a two times lower opacity than MOLIERE. Results of versatile models like MOLIERE depend on choices made by the user. At this stage, it is not clear which models fits best for data calibration, but studies to compare the AM and MOLIERE codes are under way.

In this paper, we present selected model results of MOLIERE calculated for four different altitudes (11 to 14 km in steps of 1 km), three PWVs (3, 10, and 20 μm), and a frequency range of 1800 to 2000 GHz. We chose this frequency range because it includes the astronomically very important atomic finestructure emission line of ionized carbon at 1900 GHz. Figure 9 shows the transmission curves for the four altitudes at a PWV of 10 μm. Generally, the transmission is high (>80%) except for the deep and broad water absorption features and the line absorption of minor species. Only in these ranges is the atmosphere opaque even at those high altitudes. Figure 10 shows a zoom into the frequency range around the [CII] 1.9 THz line for different PWVs. The transmission remains high (~75%) even for a PWV of 20 μm.

6. Summary and conclusions

We have presented PWV statistics and the corresponding transmission curves for potential and existing submillimetre observational sites all around the world. Thanks to satellite measurements (IASI), it is possible for the first time to conduct a comparison that is not biased by the different calibration techniques of ground-based instruments that have very different behaviours caused by their working conditions. This is particularly true for comparing polar and non-polar sites because of the harsh environmental conditions at the poles.

Comparisons were done for the PWV statistics and for the transmissions using the atmospheric model MOLIERE. For astronomical purposes, a comparison using the transmissions is mandatory since the altitude of the site also has a strong influence on the resulting transmission. For a percentage of 25% of the year, Cerro Chajnantor presents very good transmissions that are comparable to Antarctic sites. However on the long term, only Antarctic sites provide a stable transmission that will allow unique science cases to be studied there. Observations at 350 μm and 450 μm are possible all year long while the 200 μm window opens significantly for at least 25% of the year. Furthermore, Antarctic sites are free of day-night variations thanks to the long polar night. All the other sites studied here have a highly variable transmission. The typical monthly-averaged transmission at 200 μm is lower than its fluctuations on all the sites except for Domes A and C. Therefore, these two sites will be unique for surveys and time-series studies in the submm range.

The method used to compare the different sites is robust and based on only one instrument, IASI, and the atmospheric model MOLIERE. We derived the PWV and atmospheric transmission on well-known sites for submillimetre astronomy and showed that it is possible to retrieve statistics that are in good agreement with in-situ measurements. A calculator to show these PWV statistics and to compute the corresponding transmission at any given wavelength is available to the community[9] for all the sites presented here and for the three year 2008, 2009, and 2010. The year 2011 will be added to the calculator. Other potential sites could be investigated upon request.

In conclusion, this method could identify sites on Earth with a great potential for submillimetre astronomy and guide future site testing campaigns in situ.

Acknowledgements. We thank the anonymous referee for his/her comments that helped to improve this paper, in particular pointing out the importance of the pressure level for retrieving correct PWVs.

[9] http://irfu.cea.fr/submm and http://submm.eu

Appendix A: PWV statistics and transmission curves

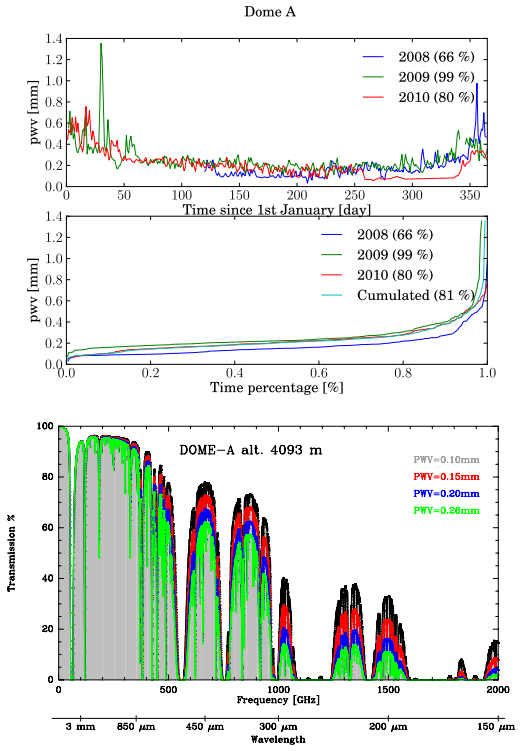

Fig. A.1. PWV statistics (*top*) and transmission curves (*bottom*) for Dome A. The transmission curve for the first decile of PWV is in grey, and the quartiles of PWV are given by red: 25%, blue: 50%, green: 75%.

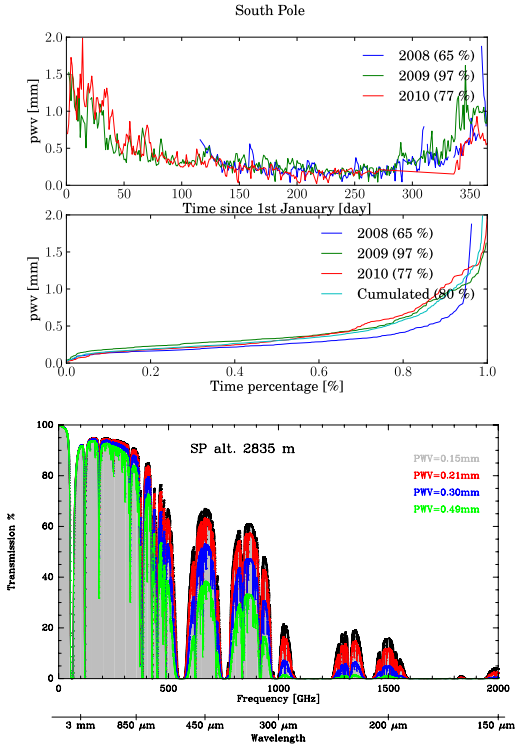

Fig. A.2. PWV statistics (*top*) and transmission curves (*bottom*) for the South Pole. The transmission curve for the first decile of PWV is in grey, and the quartiles of PWV are given by red: 25%, blue: 50%, green: 75%.

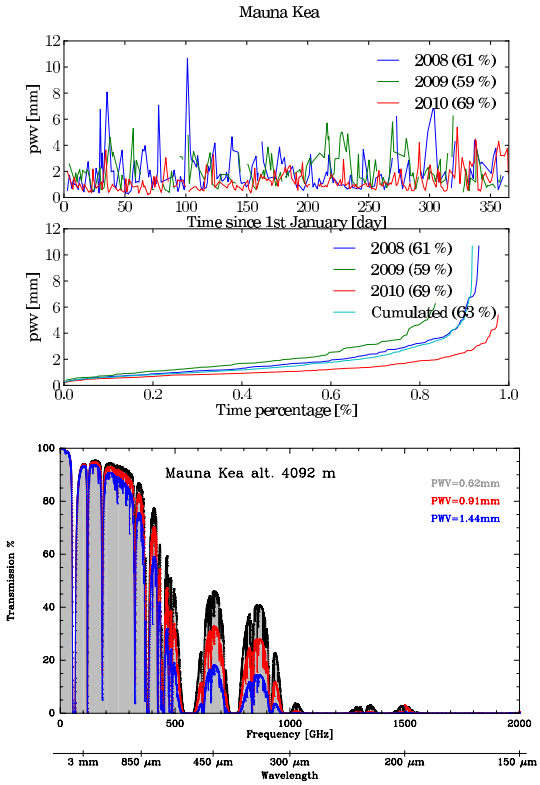

Fig. A.3. PWV statistics (*top*) and transmission curves (*bottom*) for Mauna Kea. The transmission curve for the first decile of PWV is in grey, and the quartiles of PWV are given by red: 25%, blue: 50%.

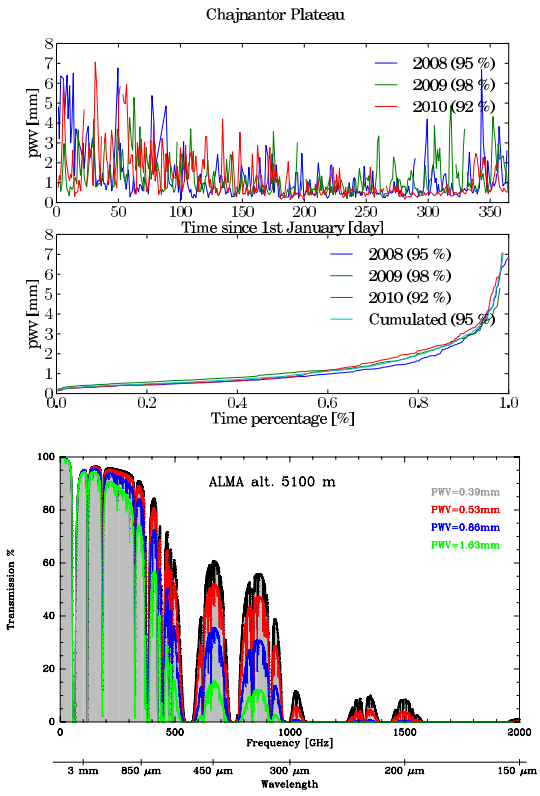

Fig. A.4. PWV statistics (*top*) and transmission curves (*bottom*) for Chajnantor Plateau. The transmission curve for the first decile of PWV is in grey, and the quartiles of PWV are given by red: 25%, blue: 50%.

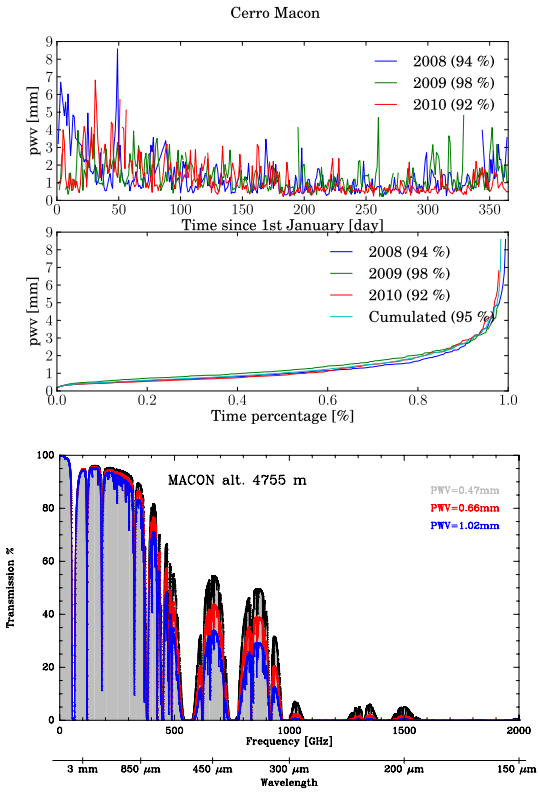

Fig. A.5. PWV statistics (*top*) and transmission curves (*bottom*) for Cerro Macon. The transmission curve for the first decile of PWV is in grey, and the quartiles of PWV are given by red: 25%, blue: 50%.

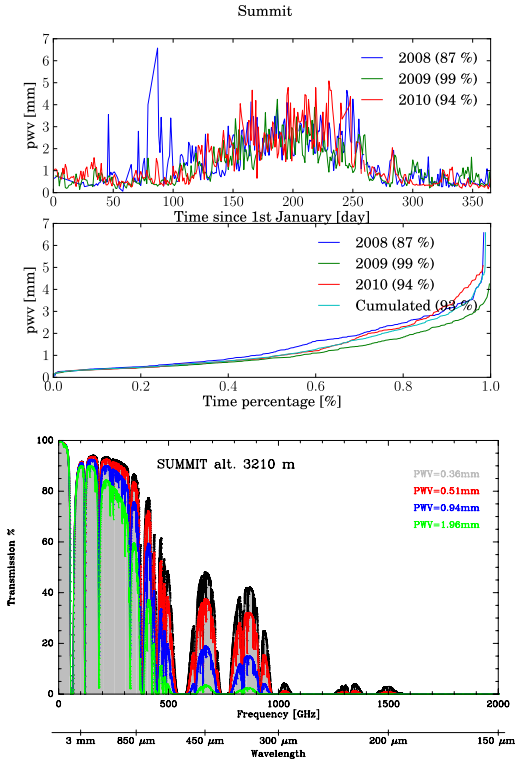

Fig. A.6. PWV statistics (*top*) and transmission curves (*bottom*) for Summit (Greenland). The transmission curve for the first decile of PWV is in grey, and the quartiles of PWV are given by red: 25%, blue: 50%, green: 75%.

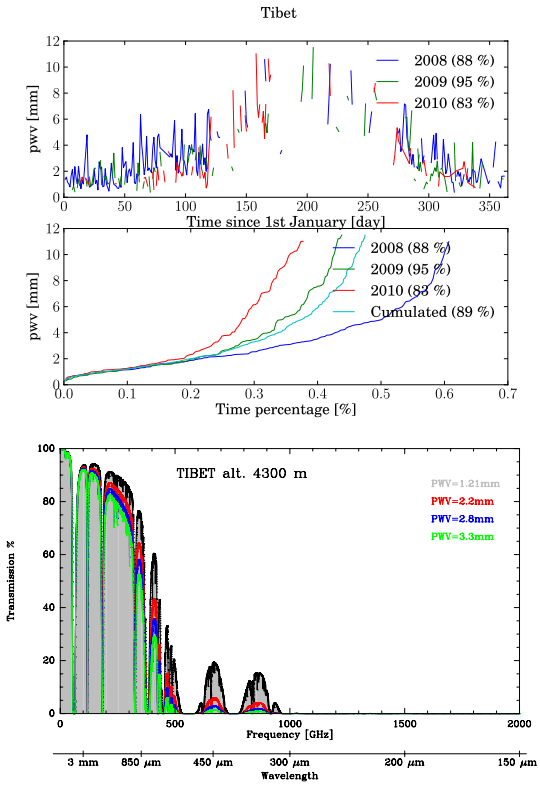

Fig. A.7. PWV statistics (*top*) and transmission curves (*bottom*) for Yangbajing (Tibet). The transmission curve for the first decile of PWV is in grey, and the quartiles of PWV are given by red: 25%, blue: 50%, green: 75%.

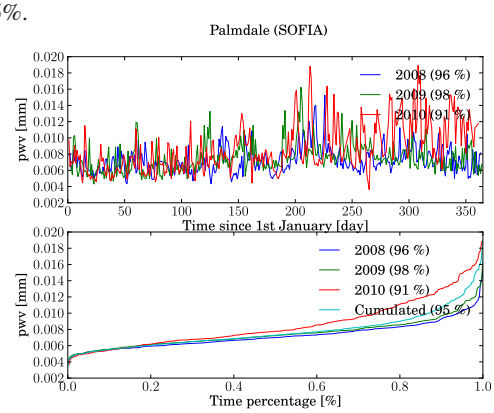

Fig. A.8. PWV statistics for Palmdale USA, at a stratospheric altitude of 12 km.

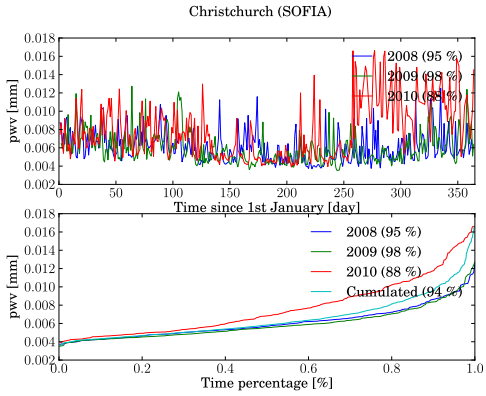

Fig. A.9. PWV statistics for Christchurch New Zealand, at a stratospheric altitude of 12 km.

References

Chamberlin, R. 2002, in Astronomical Site Evaluation in the Visible and Radio Range. ASP Conf. Proc.,266, 172
Chamberlin, R. A., Lane, A. P., & Stark, A. A. 1997, ApJ, 476, 428
Clerbaux, C., Boynard, A., Clarisse, L., et al. 2009, Atm. Chem. Phys., 9, 6041
De Gregori, S., de Petris, M., Decina, B., et al. 2012, MNRAS, 425, 222
Giovanelli, R., Darling, J., Sarazin, M., et al. 2001, PASP, 113, 789
Guan, X., Stutzki, J., Graf, U. U., et al. 2012, A&A, 542, L4
Herbin, H., Hurtmans, D., Clerbaux, C., Clarisse, L., & Coheur, P. F. 2009, Atm. Chem. Phys., 9, 9433
Matsushita, S., Matsuo, H., Pardo, J. R., & Radford, S. J. E. 1999, PASJ, 51, 603
Minier, V., Olmi, L., Durand, G., et al. 2010, in EAS Publ. Ser., 40, 269
Otárola, A., Travouillon, T., Schöck, M., et al. 2010, PASP, 122, 470
Paine, S. 2011, SMA Tech. Memo, 152
Pardo, J. R., Cernicharo, J., & Serabyn, E. 2001, IEEE Trans. Antennas Prop., 49, 1683
Peterson, J. B., Radford, S. J. E., Ade, P., et al. 2003, PASP, 115, 383
Phulpin, T., Blumstein, D., Prel, F., et al. 2007, in Atmospheric and Environmental Remote Sensing Data Processing and Utilization III: Readiness for GEOSS, ed. Goldberg, 6684, 12
Pougatchev, N., August, T., Calbet, X., et al. 2008, in Earth Observing Systems XIII, ed. Butler, 7081, 18
Radford, S. J. E. 2011, in Astronomical Site Testing Data in Chile, 41 ed. M. Curé, 87
Ricaud, P., Gabard, B., Derrien, S., et al. 2010, ITGRS, 48, 2189
Schneider, N., Urban, J., & Baron, P. 2009, PSS, 57, 1419
Tremblin, P., Minier, V., Schneider, N., et al. 2011, A&A, 535, A112
Urban, J., Baron, P., Lautié, N., et al. 2004, J. Quant. Spectr. Radiat. Transf., 83, 529
Yang, H., Kulesa, C. A., Walker, C. K., et al. 2010, PASP, 122, 490